The effect of cathode deactivation upon hydrogen evolution reaction on nickel-coated carbon fibre*

Boguslaw Pierozynski

Department of Chemistry, Faculty of Environmental Management and Agriculture, University of Warmia and Mazury in Olsztyn, Plac Lodzki 4, 10-957 Olsztyn, Poland. Phone: +48 89 523-4177; Fax: +48 89 523-4801. E-mail: bogpierozynski@yahoo.ca or boguslaw.pierozynski@uwm.edu.pl
Keywords: cathode deactivation, HER, NiCCF, nickel coated carbon fibre

ABSTRACT

The process of cathodic evolution of hydrogen at metal (or composite) electrodes is one of the most widely studied electrochemical reactions. It has important technological significance in the fields of fuel-cell and battery development. Nickel-coated carbon fibre (NiCCF) offers an attractive, large surface-area catalyst material for the process of cathodic evolution of hydrogen. Such composite materials could potentially be used to produce large area, *woven* cathodes for the generation of H_2 in commercial electrolysers. Kinetics of the hydrogen evolution reaction (HER) at commercially available NiCCF material (Toho-Tenax fibre) were studied in 30 wt.% KOH solution, at room temperature over the cathodic overpotential range: -100 to -500 mV/RHE. Significance of the *cathode deactivation* effect (in relation to the corresponding values of the charge-transfer resistance and the cathode potential parameters) upon continuous alkaline water electrolysis has also been discussed.

INTRODUCTION

The hydrogen evolution reaction (HER) has been broadly studied on noble metal catalysts, such as polycrystalline and single-crystal surfaces of Pt (Angelo 2007; Barber and Conway 1999; Barber et al. 1998; Conway and Tilak 2002; Markovic et al. 1996) and other metals and their alloys [e.g. on Ni (Hitz and Lasia 2001; Huot and Brossard 1987; Rommal and Moran 1988; Soares et al. 1992), Co (Huot and Brossard 1988), Pb (Wu et al. 2005), Zn-Ni (Sheela et al. 2002), Ni-P (Burchardt 2000; Krolikowski and Wiecko 2002) and Ni-Mo (Hashimoto et al. 2004)]. In short, the HER leads to the formation of bulk H_2 species and proceeds at potentials negative to the H_2 reversible potential. The HER mechanism at metal (Me) electrode is based on a 2-step reaction that involves an adsorbed H intermediate, as shown for alkaline media below (Barber and Conway 1999; Conway and Tilak 1992):

$$H_2O + e^- + Me \rightarrow MeH_{ads} + OH^- \quad \text{(Volmer electrochemical discharge step)} \quad (1)$$

$$MeH_{ads} + H_20 + e^- \rightarrow H_2\uparrow + OH^- + Me \quad \text{(Heyrovsky electrochemical desorption step)} \quad (2)$$

$$2MeH_{ads} \rightarrow H_2\uparrow + 2Me \quad \text{(Tafel catalytic recombination step)} \quad (3)$$

It is well-known (see e.g. works by Abouatallah et al. 2002; Huot and Brossard 1987; Rommal and Moran 1988) that catalytic metal surfaces undergo progressive deactivation towards the HER upon continuous water electrolysis. The above is usually revealed in significant increase of overpotential in time, which is attributed to reversible formation of nickel-hydride species.

Nickel-coated carbon fibre (NiCCF) composites are made by deposition of a thin layer of Ni onto the surface of carbon fibre tow. The above can be accomplished by means of chemical vapour deposition (CVD) method (Ettel et al. 1994), electroless deposition of NiP, NiB or NiP/PTFE co-deposits (Huang and Pai 1998; Huang et al. 2004; Park et al. 2002; Tzeng and Chang 2001) and an electrolytic deposition method (Morin 1986, 1987a, 1987b, 1990a, 1990b, 1990c). NiCCF could potentially offer a largely modifiable catalyst material for the HER through application of various chemical (or electrochemical) pre-treatments to CF or otherwise post-treatments applicable to NiCCF.

* Presented at The Second International Environmental Best Practices Conference, 14-18 September 2009, Krakow, Poland

The main purpose of this work is to present an introduction to the HER cathode deactivation effect, with respect to commercially available nickel-coated carbon fibre composite material, studied in highly concentrated KOH solution.

EXPERIMENTAL

Aqueous, 30 wt.% KOH solution was made up from high purity KOH pellets (POCH, Polish Chemical Compounds, p.a.), using a Direct-Q3 UV ultra-pure water (18.2 MΩ·cm resistivity) purification system from Millipore. In addition, 0.5 M H_2SO_4 solution (made up from high purity sulphuric acid, Fluka) was used for electrochemical activation of NiCCF tow electrodes.

An electrochemical cell made of an HDPE material was used during the course of this work. The cell comprised three electrodes: a nickel-coated carbon fibre working electrode (WE) in a central part, a reversible Pd hydrogen electrode (RHE) as reference and a Pt counter electrode (CE), both in separate compartments. Atmospheric oxygen was removed from solution before each experiment by bubbling with high-purity Ar (Eurogas, grade 5.0). During the experiments, the argon gas flow was usually kept above the solution.

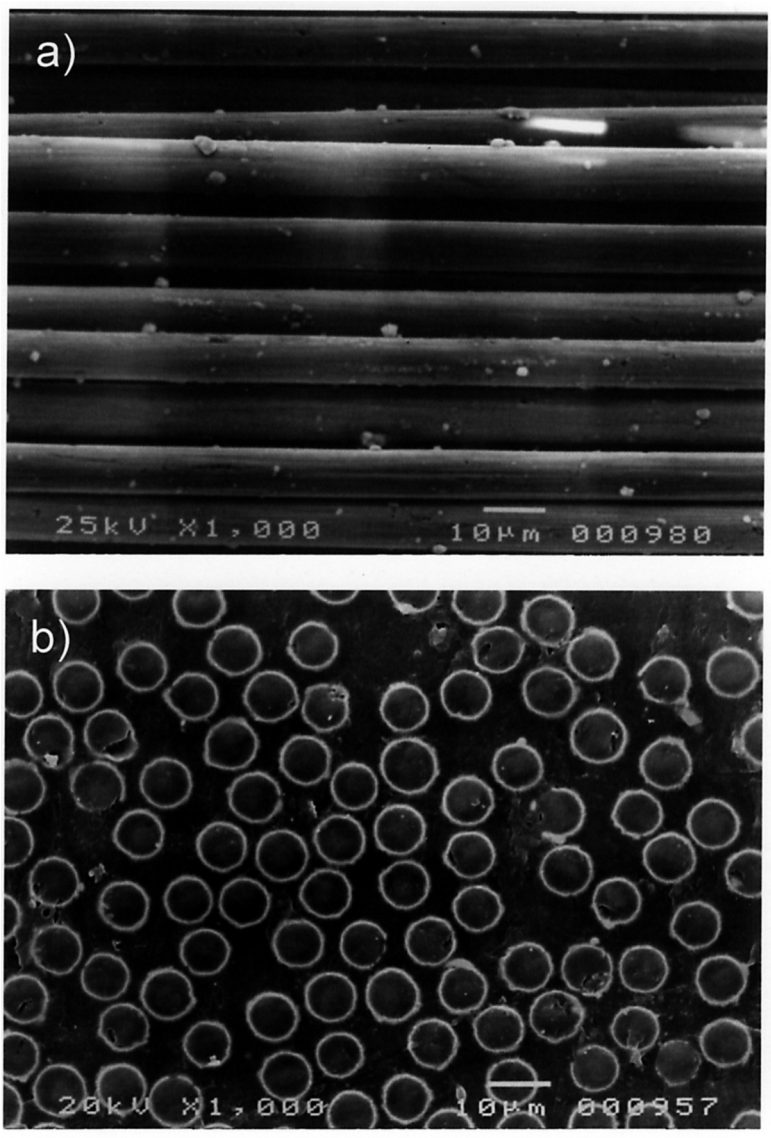

Figure 1. a) SEM micrograph picture of Toho-Tenax electrodeposited NiCCF sample (46 wt.% Ni), taken at 1,000 magnification [powder XRD-calculated Ni grain size for this material came on average to ca. 25 nm (Pierozynski and Smoczynski 2008)], and b) cross-sectional sample view, taken at 1,000 magnification.

All experiments were carried-out on a commercially available, electro-deposited (ca. 45 wt.% Ni) 12K50 NiCCF product from Japanese Toho-Tenax company (Toho-Tenax website 2010), where 12K50 refers to 12,000 single filament tow, 7 micron diameter each, with a thickness of Ni layer of ca. 0.3 μm.

A.c. impedance spectroscopy, cyclic voltammetry and galvanostatic/potentiostatic polarization techniques were employed during the course of this work. All measurements were conducted at room temperature by means of the Solartron 12608W Full Electrochemical System, consisting of 1260 frequency response analyzer (FRA) and 1287 electrochemical interface (EI). For potential-controlled impedance measurements, the generator provided an output signal of known amplitude (5 mV) and the frequency range was typically swept between 100 kHz and 50 mHz. The instruments were controlled by ZPlot 2.9 or Corrware 2.9 software for Windows (Scribner Associates, Inc.).

RESULTS AND DISCUSSION

Hydrogen evolution reaction at Toho-Tenax NiCCF in 30 wt.% KOH solution

A sample of Toho-Tenax nickel-coated carbon fibre is shown in SEM pictures of Figures 1a and 1b. It can be seen there that the nickel deposit is fairly homogeneous throughout the tow (specifically evidenced in the cross-sectional tow view shown in Figure 1b).

The a.c. impedance characterization of the HER at Toho-Tenax electrodeposited 12K50 NiCCF electrodes in 30 wt.% KOH revealed single and "depressed" semicircles (obtained complex-plane impedance plots are not shown in this work) for all successive polarization cycles, studied at five selected overpotentials in the explored frequency range. The above behaviour is characteristic of a single-step charge-transfer

reaction, proceeding on non-homogeneous/non-uniform electrode surfaces. Therefore, a constant phase element – CPE modified Randles equivalent circuit model (see e.g. work by Daftsis et al. 2003 and Figure 2) was used to derive all electrochemical parameters.

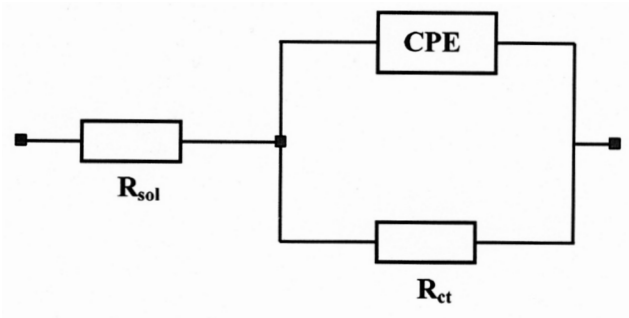

Figure 2. Equivalent circuit model used for fitting the impedance data for Toho-Tenax 12K50 NiCCF tow electrodes, obtained in 30 wt.% KOH solution. The circuit exhibits a Faradaic charge-transfer resistance (R_{ct}) in a parallel combination with the double-layer capacitance (C_{dl}) [represented by the constant phase element (CPE) for distributed capacitance], jointly in series with an uncompensated solution resistance (R_{sol}).

The electrochemical performance of Toho-Tenax NiCCF material towards the HER in 30 wt.% KOH solution was independently studied on three 12K50 tow electrodes, at room temperature, over the period of 3 days. Thus, cathodically activated in 0.5 M H_2SO_4 (by cathodic polarization at a current-density of 1 mA·cm^{-2} for 900 s) Toho fibre electrodes were subjected to three consecutive, 24-hour cathodic polarization cycles (at the cathodic current-density of -0.5 mA·cm^{-2}). The reaction resistance (Rct) for the HER was measured before and after each galvanostatic polarization cycle. The dependence of an average value of the Rct parameter (where Rct typically varied ± 5 % for each potential between experimental series) on applied overpotential, for initial 48 hours of electrolysis, is presented in Figure 3. Thus, originally the charge-transfer resistance parameter ranges from 0.218 Ω·g (recorded at -100 mV) to 0.004 Ω·g for the potential of -500 mV/RHE (see Figure 3).

It can also be observed in Figure 3 that the Rct parameter significantly (and progressively) increases during the time that cathodic polarization is carried-out, for all overpotential values. For example, after 24 hours of continuous electrolysis, the Rct parameter has increased ca. 2.4 and 5.2 times at -200, and -300 mV, correspondingly. Furthermore, 48 hours of galvanostatic electrolysis led to an increase of the Rct parameter by 3.8 and 12.9 times for the respective (-200 and -300 mV) overpotentials. Moreover, the HER experiments (performed galvanostatically at the cathodic current-density of -0.5 mA·cm^{-2}) explicitly showed (see Figure 4) that the NiCCF cathode undergoes considerable polarization (from about -240 mV to ca. -450 mV vs. Pd RHE) during initial 72 hours of H_2 generation.

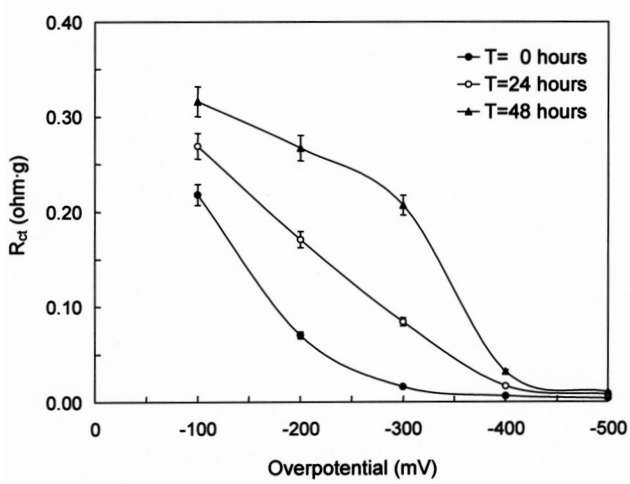

Figure 3. Changes of the Rct parameter for Toho-Tenax NiCCF tow cathode during the cathodic polarization experiment (recorded for 5 selected overpotentials, with an error less than ± 5% for the three indicated experimental series).

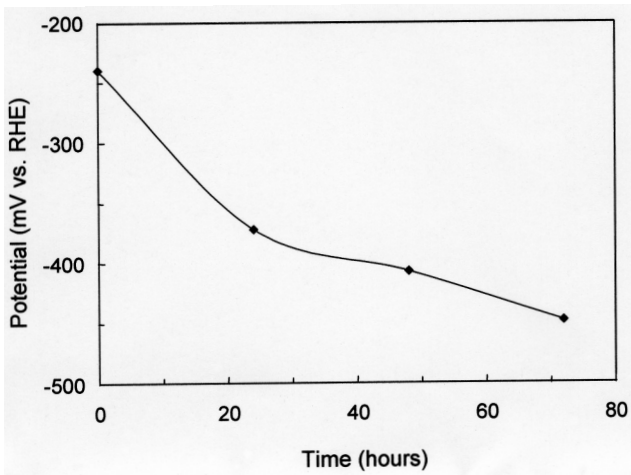

Figure 4. Changes of Toho-Tenax NiCCF cathode potential (IR corrected) during the galvanostatic (j_c= -0.5 mA·cm^{-2}) HER cathodic polarization experiment.

These results indicate that NiCCF cathodes undergo significant deactivation upon continuous alkaline water electrolysis. The above is likely due to extensive formation of NiH species (see equations 4 and 5 below), as previously suggested in other works, see for example (Baer et al. 1997; Bernardini et al. 1998; Brass and Chanfreau 1996; Highfield et al. 1999; Juskenas et al. 2002; Nishimura et al. 2007; Santos and Miranda 1998; Vracar and Conway 1990).

$$NiH_{ads} + Ni_{subsurf} \rightarrow NiH_{abs\,/\,subsurf} + Ni_{surf.}$$
(H absorption/sub-surface Ni layer) (4)

$$NiH_{abs\,/\,subsurf} \rightarrow NiH_{abs\,/\,bulk}$$
(further H diffusion into bulk Ni) (5)

Similar findings have recently been reported by Pierozynski and Smoczynski (2008, 2009) with respect to the HER studied on various NiCCFs in 0.5 M H_2SO_4 and 0.1 M NaOH solutions. There, extensive cathodic polarizations (upon a.c. impedance measurements) led to dramatic cathode deactivation, yielding Tafel slopes on the order of 250 (in acidic) and up to 400 mV·decade^{-1} (in alkaline) electrolytes.

In-situ, cyclic voltammetry reactivation of NiCCF cathode

Electrochemically deactivated Toho-Tenax electrodes (via potentiostatically-controlled HER, carried-out with the cathode set at -0.5 V/RHE for one hour) were then subjected to a cyclic voltammetry treatment involving CV scanning over the potential range 0.0 to 1.0 V (Figure 5). Thus, an initial part of the cyclic voltammetric profile shown in Figure 5 reveals an anodic oxidation peak at the potential range ca. 0.1 through 0.5 V. This is reminiscent of the process of anodic hydrogen oxidation reaction that proceeds over the stated potential range. Then, this peak disappears as the NiCCF cathode is continuously cycled within the potential range that is positive to the H_2 reversible potential (Figure 5).

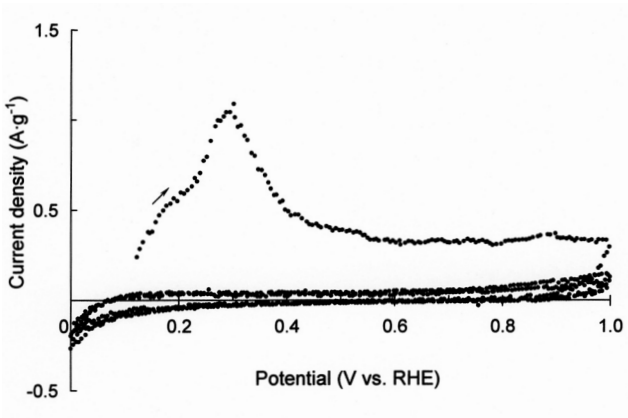

Figure 5. Cyclic voltammetry reactivation of Toho-Tenax NiCCF electrode in 30 wt.% KOH, recorded at a sweep rate of 50 mV·s^{-1} over the potential range 0.0-1.0 V/RHE.

The above-made conclusions get strong support from evaluations of the charge-transfer resistance parameter (Table 1), derived in a sequence for: a) fresh, b) deactivated and c) CV-reactivated (as in Figure 5) Toho-Tenax NiCCF electrode. Thus, the Rct values recorded for a deactivated cathode were ca. 5.7, 2.4 and 1.6 times as high as those recorded for a fresh one, at -100, -200 and -300 mV/RHE, correspondingly. Conversely, the CV treatment leads practically to complete electrochemical reactivation of the electrode, with the set of the charge-transfer resistance values on the order of those characteristic of the fresh electrode surface (compare the CV-reactivated values of the Rct parameter with those of the fresh electrode in Table 1).

In addition, the double-layer capacitance (C_{dl}) parameter (recorded for an activated NiCCF electrode at the potential of -100 mV) came to ca. $2.0 \cdot 10^5$ $\mu F \cdot g^{-1} \cdot s^{\varphi-1}$ (about 90 $\mu F \cdot cm^{-2}$). Simultaneously, the dimensionless φ parameter (φ determines the constant-phase angle in the complex-plane plot and $0 \leq \varphi \leq 1$) of the CPE circuit (Daftsis et al. 2003) oscillated around 0.85-0.90. Both parameters are on the order of those recently reported (Pierozynski and Smoczynski 2009) for Toho-Tenax NiCCF in 0.1M NaOH solution. On the other hand, the Cdl parameter values for both deactivated and the CV-reactivated NiCCF electrode came to ca. $5.0 \cdot 10^5$ $\mu F \cdot g^{-1} \cdot s^{\varphi-1}$, which was 2.5· the C_{dl} value for the freshly activated electrode (the dimensionless φ parameter values followed those recorded for the fresh electrode). A substantial increase in the double-layer capacitance could imply significant surface roughening, the effect of extended cathodic polarization of the NiCCF electrode.

CONCLUSIONS

- Prolonged cathodic polarizations of the 12K50 Toho-Tenax composite tow electrode, carried-out in 30 wt.% KOH solution, lead to severe deactivation of electrode surfaces, brought about by the reversible formation of nickel hydride species.
- Such-deactivated NiCCF electrode could become successfully reactivated by the process of in-situ hydrogen oxidation upon cyclic voltammetry sweep, over the potential range 0.1-0.5 V/RHE. The above process requires further and detailed investigation, especially with respect to the long-term polarization behaviour of NiCCF material(s) and possible application of other in-situ electrode reactivation procedures.

Table 1. Variation of the charge-transfer resistance (R_{ct}) parameter for the HER on: fresh, deactivated and CV-reactivated Toho-Tenax NiCCF electrode in 30 wt.% KOH, obtained by fitting the equivalent circuit (Daftsis et al. 2003 and Figure 2) to the experimentally obtained impedance data, for selected overpotentials.

E/mV	Rct/Ω·g (fresh)	Rct/Ω·g (deactivated)	Rct/Ω·g (CV-reactivated)
-100	0.150 ± 0.001	0.855 ± 0.010	0.129 ± 0.001
-200	0.059 ± 0.000	0.142 ± 0.001	0.056 ± 0.001
-300	0.015 ± 0.000	0.024 ± 0.001	0.015 ± 0.000

REFERENCES

Abouatallah, R.M., D.W. Kirk, J.W. Graydon. 2002. Long-term electrolytic hydrogen permeation in nickel and the effect of vanadium species addition. Electrochimica Acta 47: 2483-2494.

Angelo, A.C.D. 2007. Electrocatalysis of hydrogen evolution reaction on Pt electrode surface-modified by S-2 chemisorption. International Journal of Hydrogen Energy 32: 542-547.

Baer, R, Y. Zeiri, R. Kosloff. 1997. Hydrogen transport in nickel (111). Physical Review B 55: 10952-10974.

Barber, J.H., B.E. Conway. 1999. Structural specificity of the kinetics of the hydrogen evolution reaction on the low-index surfaces of Pt single-crystal electrodes in 0.5 M NaOH. Journal of Electroanalytical Chemistry 461: 80-89.

Barber, J.H., S. Morin, B.E. Conway. 1998. Specificity of the kinetics of H_2 evolution to the structure of single-crystal Pt surfaces, and the relation between opd and upd H. Journal of Electroanalytical Chemistry 446: 125-138.

Bernardini, M., N. Comisso, G. Davolio, G. Mengoli. 1998. Formation of nickel hydrides by hydrogen evolution in alkaline media. Journal of Electroanalytical Chemistry 442: 125-135.

Brass, A.M., A. Chanfreau. 1996. Accelerated diffusion of hydrogen along grain boundaries in nickel. Acta Materialia 44: 3823-3831.

Burchardt, T. 2000. The hydrogen evolution reaction on NiP_x alloys. International Journal of Hydrogen Energy 25: 627-634.

Conway, B.E., B.V. Tilak. 1992. Behavior and characterization of kinetically involved chemisorbed intermediates in electrocatalysis of gas evolution reactions. Advances in Catalysis 38: 1-147.

Conway, B.E., B.V. Tilak. 2002. Interfacial processes involving electrocatalytic evolution and oxidation of H_2, and the role of chemisorbed H. Electrochimica Acta 47: 3571-3594.

Daftsis, E., N. Pagalos, A. Jannakoudakis, P. Jannakoudakis, E. Theodoridou, R. Rashkov, M. Loukaytsheva, N. Atanassov. 2003. Preparation of a carbon fiber-nickel-type material and investigation of the electrocatalytic activity for the hydrogen evolution reaction. Journal of The Electrochemical Society 150: C787-C793.

Ettel, V.A., E. Krause, J. Van Wagner. 1994. Metal coating of inorganic fibers and solid particulates. Canadian Patent 1 333 547.

Hashimoto, K., T. Sasaki, S. Meguro, K. Asami. 2004. Nanocrystalline electrodeposited Ni-Mo-C cathodes for hydrogen production. Materials Science and Engineering A 375-377: 942-945.

Highfield, J.G., E. Claude, K. Oguro. 1999. Electrocatalytic synergism in Ni/Mo cathodes for hydrogen evolution in acid medium: a new model. Electrochimica Acta 44: 2805-2814.

Hitz, C., A. Lasia. 2001. Experimental study and modeling of impedance of the her on porous Ni electrodes. Journal of Electroanalytical Chemistry 500: 213-222.

Huang, C.Y., J.F. Pai. 1998. Optimum conditions of electroless nickel plating on carbon fibres for EMI shielding effectiveness of ENCF/ABS composites. European Polymer Journal 34: 261-267.

Huang, C.Y., W.W. Mo, M.L. Roan. 2004. Studies on the influence of double-layer electroless metal deposition on the electromagnetic interference shielding effectiveness of carbon fiber/ABS composites. Surface and Coatings Technology 184: 163-169.

Huot, J.Y., L. Brossard. 1987. Time dependence of the hydrogen discharge at 70°C on nickel cathodes. International Journal of Hydrogen Energy 12: 821-830.

Huot, J.Y., L. Brossard. 1988. In situ activation of cobalt cathodes in alkaline water electrolysis. Journal of Applied Electrochemistry 18: 815-822.

Juskenas, R., R. Giraitis, V. Pakstas. 2002. X-ray diffraction investigation of nickel-hydride formation in alkaline solution. Chemija 13: 26-31.

Krolikowski, A., A. Wiecko. 2002. Impedance studies of hydrogen evolution on Ni-P alloys. Electrochimica Acta 47: 2065-2069.

Markovic, N.M., S.T. Sarraf, H.A. Gasteiger, P.N. Ross. 1996. Hydrogen electrochemistry on platinum low-index single-crystal surfaces in alkaline solution. Journal of Chemical Society, Faraday Transaction 92: 3719-3725.

Morin, L.G. 1986. Apparatus for the production of continuous yarns or tows comprising high strength metal coated fibers. US Patent 4 609 449.

Morin, L.G. 1987a. Yarns and tows comprising high strength metal coated fibers, process for their production, and articles made therefrom. US Patent 4 661 403.

Morin, L.G. 1987b. Metal bonded composites and process. US Patent 4 680 093.

Morin, L.G. 1990a. Yarns and tows comprising high strength metal coated fibers, process for their production, and articles made therefrom. US Patent 4 909 910.

Morin, L.G. 1990b. Chaff comprising metal coated fibers. US Patent 4 942 090.

Morin, L.G. 1990c. Chaff comprising metal coated fibers. US Patent 4 976 828.

Nishimura, R., H. Inoue, K. Okitsu, R.M. Latanision, G.K. Hubler. 2007. Hydrogen permeation behavior in pure nickel implanted with phosphorus, sulphur and their mixture. Corrosion Science 49: 1478-1495.

Park, S.J., Y.S. Jang, K.Y. Rhee. 2002. Interlaminar and ductile characteristics of carbon fibers-reinforced plastics produced by nanoscaled electroless nickel plating on carbon fiber surfaces. Jornal of Colloid and Interface Science 245: 383-390.

Pierozynski, B., L. Smoczynski. 2008. Electrochemical corrosion behavior of nickel-coated carbon fiber materials in various electrolytic media. Journal of The Electrochemical Society 155: C427-C436.

Pierozynski, B., L. Smoczynski. 2009. Kinetics of hydrogen evolution reaction at nickel-coated carbon fiber materials in 0.5 M H_2SO_4 and 0.1 M NaOH solutions. Journal of The Electrochemical Society 156: B1045-B1050.

Rommal, H.E.G., P.J. Moran. 1988. The role of absorbed hydrogen on the voltage-time behavior of nickel cathodes in hydrogen evolution. Journal of The Electrochemical Society 135: 343-346.

Santos, D.S.D., P.E.V.D. Miranda. 1998. Hydrogen solubility in amorphous and crystalline materials. International Journal of Hydrogen Energy 23: 1011-1017.

Sheela, G., M. Pushpavanam, S. Pushpavanam. 2002. Zinc-nickel alloy electrodeposits for water electrolysis. International Journal of Hydrogen Energy 27: 627-633.

Soares, D.M., O. Teschke, I. Torriani. 1992. Hydride effect on the kinetics of the hydrogen evolution reaction on nickel cathodes in alkaline media. Journal of The Electrochemical Society 139: 98-105.

Wu, Y.M., W.S. Li, X.M. Long, F.H. Wu, H.Y. Chen, J.H. Yan, C.R. Zhang. 2005. Effect of bismuth on hydrogen evolution reaction on lead in sulfuric acid solution. Journal of Power Sources 144: 338-345.

Tenax®MC HTA A302. Nickiel-coated filament yarn. Material Safety Data Sheet. 2010. http://www.tohotenax-eu.com.

Tzeng, S.S., F.Y. Chang. 2001. EMI shielding effectiveness of metal-coated carbon fiber-reinforced ABS composites. Materials Science and Engineering A302: 258-267.

Vracar, L., B.E. Conway. 1990. Hydride formation at Ni-containing glassy-metal electrodes during the H_2 evolution reaction in alkaline solutions. Journal of Electroanalytical Chemistry 277: 253-275.